

# Satellite Photometric Error Determination

**Tamara E. Payne, Philip J. Castro, Stephen A. Gregory**

*Applied Optimization*

*714 East Monument Ave, Suite 204*

*Dayton, OH 45402*

**Phan Dao**

*AFRL/RVBY*

*3550 Aberdeen Ave. SE*

*Kirtland, AFB, NM 87117-5776*

## ABSTRACT

In this paper, we present analysis of the errors associated with optical photometry used in non-resolved object characterization for the Space Situational Awareness (SSA) community. We begin with an overview of the standard astronomical techniques used to measure the brightness of spatially unresolved objects (point source photometry) in deep space. After discussing the standard astronomical techniques, we present the application of astronomical photometry for the purposes of space object characterization. Examples of filter photometry of geosynchronous satellites processed using the current techniques are shown. Next we advocate the adoption of new techniques based on in-frame photometric calibrations enabled by newly available all-sky star catalogs that contain highly accurate photometry.

## 1. INTRODUCTION

Over the years, photometry has progressed from visual to photographic to photoelectric to modern solid state detectors with accompanying improvements and refinements in filter technology. We are at a crossroads now in which the standard set of Johnson based filter systems will likely be supplanted by the Sloan based filter systems.

The Johnson photometric system is a set of filters in the optical wavelength region; the UBV spectral regions were established by [1], and [2] later added the RI spectral regions [3]. An additional RI system was also defined by [4], and [5] later modified this RI system [6]. The final definition of the Johnson-Cousins standard system (UBVR<sub>c</sub>I<sub>c</sub>) is the result of extensive work by Arlo Landolt [7]. He published a list of standard stars in the UBV system and [6] extended this list to include stars in the Cousins R and I bands. Most astronomers use Landolt standard stars to transform their system to that of the Johnson-Cousins system [8]. The Johnson photometric system has been used by the astronomical community for decades [7] [6] [9] [10] [11]. For a more thorough discussion of the development and evolution of the Johnson system see [6] and [3]. This photometric system has historically been used for filter observations of satellites [12] [13], and we discuss those applications in Section 2. The calibration of satellite observations using the Johnson photometric system requires calibration stars in the same system – i.e. secondary standard stars that have been observed via the same filters and whose relationship to primary standard stars has been well established. Recent calibration star catalogs include Landolt standard stars [10] [11], as well as secondary standards from Stetson [14] and near secondary standards from Henden [8]. In order to standardize filter photometry across sites and telescopes, a common calibration star catalog should be implemented. A standardization of the filters themselves should also be taken into consideration. Variations upon the R and I band passes of the Johnson system still exist today in filter sets. An attempt to standardize a filter set in the optical for the Johnson photometric system could have an analogous impact to the SSA community as the standardization of a filter set in the infrared did to the astronomical community with the Mauna Kea Observatory (MKO) infrared photometric system

established by [15] [16] [17]. The MKO infrared filter set has been accepted by the astronomical community as the new standard pass bands and most observatories are now using these filters [3]. Without standardization of filter photometry across sites and telescopes, the ability to accurately compare data between sites and telescopes is in question.

All-sky, or absolute, photometry performs calibrations by (logically if not actually) following a group of calibration stars in a single frame across as large a range of air mass as possible. The effectiveness of all-sky photometry requires that conditions do not change significantly while the calibration data is being collected; this is rare for all but the better observing locations [8]. Landolt standard star catalogs, or derivative subsets, are often used for all-sky photometric calibrations. However, these catalogs are sparse and the number of stars is small; therefore they cannot serve as in-frame calibrations for observations with typical small telescopes.

As a very rough assessment of the accuracies that have been achieved during the progression of detector technologies that we discussed above, we note the following: The uncertainty of visual photometry is on the order of  $\pm 1.0$  magnitude. Photographic techniques yield accuracies of  $\pm 0.3$  magnitudes. Typical photoelectric techniques produce accuracies of  $\pm 0.05$  magnitudes or better, and with intensive effort, accuracies in the astronomical community today may often approach  $\pm 0.001$  magnitudes.

Standard astronomical community techniques for extracting photometry from raw CCD images have evolved over the last 30 years or so. They typically include the following basic steps:

- Bias subtraction using
  - Overscan region, or
  - Median filtered superbias constructed from many individual bias frames.
- Dark current subtraction obtained from median filtered superdark constructed from many zero illumination frames with proper exposure times.
- Flat fielding using either
  - Twilight sky observations,
  - Out of focus uniformly-illuminated screen attached to inside of the telescope enclosure, or
  - Median filtered target frames when enough background sky counts are available.
- Additional processing is required for wide field of view telescopes with mosaic detectors.

## 2. CURRENT CALIBRATION PRACTICES FOR SSA OBSERVATIONS

### 2.1 Rationale

When the authors began photometric work on satellites in Geosynchronous Earth Orbit (GEO) two decades ago, the standard modes of observing Resident Space Objects (RSOs) featured the following:

- Little or no calibration via standard stars,
- Unfiltered photometry,
- Synoptic tasking and collections not considered,
- Seasonal brightness changes known empirically but lacked an analytical expression, and
- Inability to compare data from one sensor to another.

Under Air Force Research Laboratory sponsorship, Gregory and Payne began observations that led to the GEO Color Photometry Catalog (GCPC) that tried to remedy some of the problems listed above for geostationary satellites. In particular, we emphasized the needs for effective calibrations and for the use of photometric filters so that color indices, as well as brightness, could be used to derive additional intrinsic satellite features for characterization. In these early versions of the GCPC, we were able to demonstrate the following capabilities that were not possible with photometry with large uncertainties [18] [19] [20] [21] [22] [23].

- Signature classes – a strong relationship exists between the photometry and the manufacturer/bus type

- Feature extraction
- Cross-tagging resolution
- Anomaly analysis

Our goals in the collection of GEO photometric observations have been the following:

- High levels of photometric accuracy
- Exploration of which filter band passes are most useful
- High level of automation
- Efficient data reduction, data analysis, and data cataloging methods

Our goals for non-resolved space object characterization have been the following:

- Develop methods for space-based observations
- Collection of color photometry signatures of all Geostationary objects over the continental US
- Develop new feature extraction methods such as albedo-area measurements
- Understanding of seasonal variations
- Ability to compare photometric observations of the same objects from multiple sensors

An important factor affecting all of these goals is the level of accuracy that is required in order to perform non-resolved object characterization. By accuracy we mean photometric observations with low uncertainties transformed to a standard magnitude system. Producing accurate photometry is not a simple task. The real-world necessities of working with multiple partners and sensors in flexible networks offers significant advantages in assuring clear-sky coverage, examining seasonal effects, and combining data, but the addition of sensors takes away certain aspects of control – particularly in the area of calibrations.

To be specific, calibrations would ideally include the following:

- Detector characterization (bias, darks, flats)
- Effective spectral band pass characterization
- Data collected in less than photometric conditions

In the real world situation of a variety of modest-sized sensors working either individually or in networks, we find that different sensors have different levels of detector and filter characterization. Additionally, different observers interpret the need for “photometric skies” differently, and there are differing opinions on what is the best practice for collecting biases, darks, and flat fields.

In our own current data reduction procedures, we deviate from the standard astronomy community methods out of necessity. We note that the specific techniques discussed here may differ in detail from those of other research groups using small telescopes; however, the general methods are often quite similar.

## **2.2 In Frame Corrections**

As an example of our procedural compromises, we do not perform the standard frame level corrections – bias subtraction, dark subtraction, and use of standard combined frames for flat-fielding purposes. In our data processing, we combine all of these steps by constructing a model based on each frame for overall corrections. Using this type of technique bypasses the dependency of the image processing on the observer’s correct collection of bias, darks, and flat field images.

Our background-correction method is illustrated in Fig. 1- Fig. 3. In Fig. 1, we present an inverse display of the raw data from a CCD observation taken of a GEO satellite (with another GEO in the upper left hand corner). The observation was made on June 26, 2014 using a 16-inch telescope with an 8 second exposure taken in the Johnson B filter.

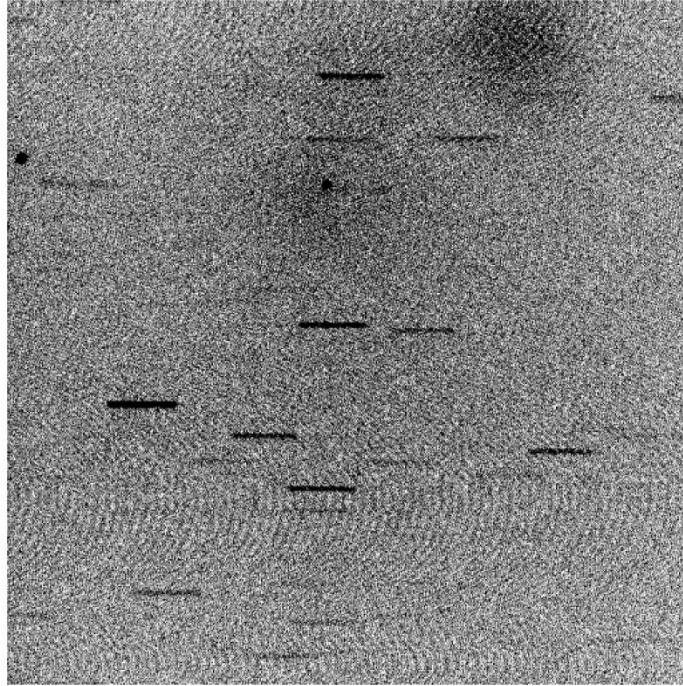


Fig. 1 Raw B filter observation of a GEO satellite taken using a small telescope

In Fig. 1, one can easily see two kinds of flaws in the raw image. There are low spatial frequency bright patches located in the upper portion of the data frame. There are also high spatial frequency patterns seen both near the top and bottom edges and about a fifth of the way up in this image. In principle, well-constructed flat field frames could remove both kinds of flaw. However, current methods only remove the low spatial frequency effects.

Our current method is to use the MATLAB<sup>1</sup> “interp2” function (with ‘spline’ option) to fit a 2-D representation of a smoothed image. The interpolation fitting is made to the median values in 25 x 25 pixel regions in the raw data. We have tried several other roughly similar methods and find that this one works well. Note that this method does not allow for adequate flattening of the edges of the field.

Fig. 2 illustrates the flattening calculation for the chosen example. This image corresponds well to the intuitive analysis of the background in Fig. 1.

---

<sup>1</sup> [www.mathworks.com](http://www.mathworks.com)

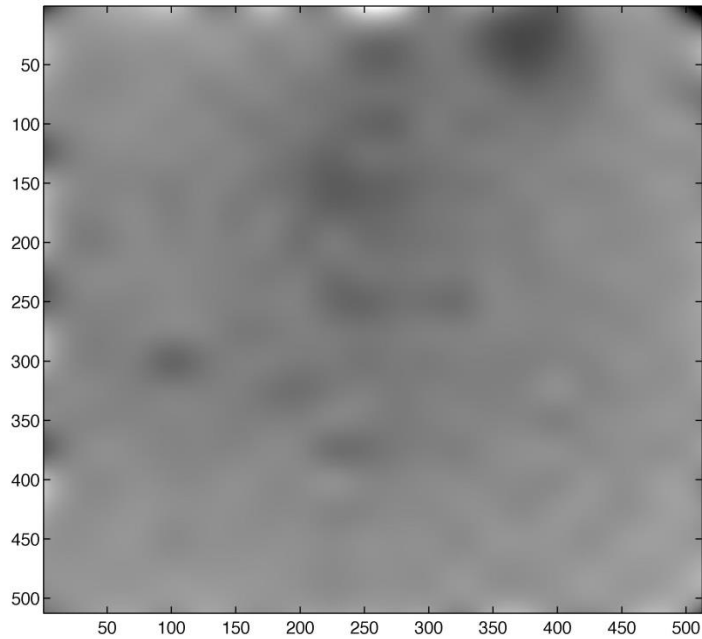


Fig. 2 The 2-D interpolated background correction for the image shown in Fig. 1

Once the background correction has been calculated, then it is subtracted from the raw image. Fig. 3 illustrates the final processed image that is used to extract the photometry. We note that the low spatial frequency problems appear to be mitigated, but the high spatial frequency issues have not been corrected. We have experimented with 2-D Fourier techniques for cleaning up the high spatial frequency problems, but we have not put these methods into production yet.

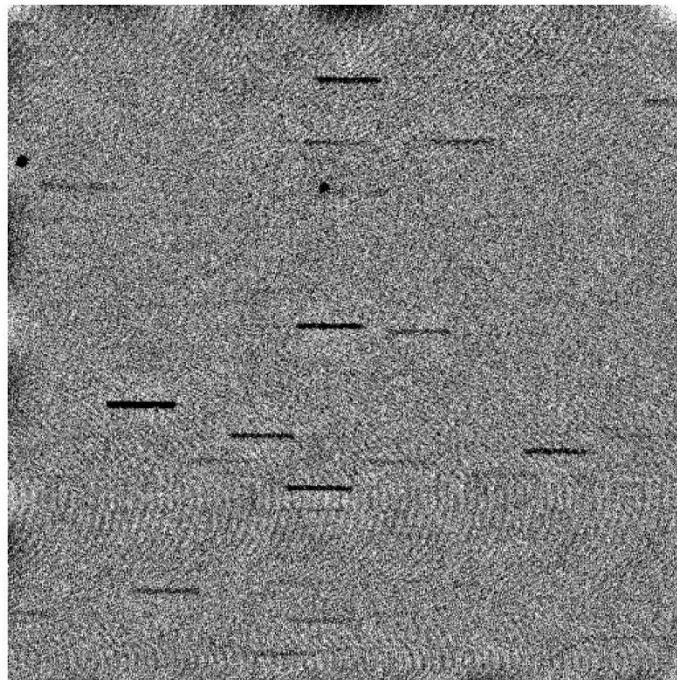


Fig. 3 The final image after the background corrections have been applied

### 2.3 All Sky Calibrations

At this time, we do not attempt to use in-frame stellar calibrations. Instead, we perform all-sky calibrations using a catalog based on Landolt (1992). This catalog was later refined by A. Henden (private communication) and further refined by S. Gregory, T. Payne, and F. Vrba [22].

We usually find 30 to 100 calibration star observations per night to determine mean or median values of  $C_i$  (the nightly zero point offset between catalog and instrumental magnitudes in the  $i^{\text{th}}$  filter). All magnitude calculations for standard stars are carried out similarly to those of the GEO satellites.

For the  $k_i$  corrections (atmospheric extinction in the  $i^{\text{th}}$  filter), we take a full night of calibration data and use it as the seasonal mean or median values for a month or so at a time. We note that many workers use extinctions calculated on a nightly basis with small sets of calibration data. But we have found that taking a full night of calibration data every month or so results in smaller uncertainties than when a small amount of calibration data is taken on a nightly basis. It takes considerable sensor time to take the calibration data nightly and since enough calibrations cannot be collected to improve the uncertainties, the overall magnitude uncertainties in the atmospheric correction are higher using this approach.

This highlights the problem with using the all sky calibration method. Even after all the effort and sensor time, there is no guarantee that the atmospheric extinction value that is used is representative of the actual true atmosphere at the time of the satellite observation. An in-frame calibration method should address this shortcoming.

### 2.4 Photometric Extraction

One of the authors (Gregory) uses Source Extractor<sup>2</sup> (SE) as a method of finding RSO and star images within our data frames. Gregory's method is discussed here. Other authors, such as Payne and Castro, use PyRAF<sup>3</sup> in a similar way. We employ a multi-pass technique – mainly because this method allows association of the satellite to the observation and to reject the spurious detections that are common to all automated extraction techniques, e.g. cosmic ray detections.

In Pass 1, the Pre-Process phase, we run SE through all images obtained for a given mount pointing in one night. The number of different images for each Field of View (FOV) is typically between 200 and 1,000. There are frequently multiple satellites in each frame. At the end of Pass 1, the user sees a plot of all row, column coordinates for every image that SE detected that satisfies the criteria for being a GEO (generally round images since telescope is tracking at the rate of the GEO, while the stars are streaks). Typically, there are a few spurious detections as well as one to three valid satellite detections in each frame, but the spatial distribution of the spurious images is generally not spatially correlated while the GEO detections are highly correlated. Therefore, the user defines a box-shaped pixel Region of Interest (RoI) that includes the GEO in question and rejects other satellites and most spurious detections.

In Pass 2, the Photometry phase, all images are again run through SE. This time all detections within the RoI go through the process of having their magnitudes calculated. Our method is to use the flux found by SE in order to calculate the instrumental magnitude of the object. The  $C_i$  and  $k_i$  corrections are applied and the result is the best estimate we can make for the exo-atmospheric magnitude of the object. An additional set of calculations is performed at this time in order to determine the solar phase angles. We calculate the total phase angle and its latitudinal (north-south) and longitudinal (east-west) components.

In Pass 3, the Cleanup phase, we plot the color signatures (typically Johnson B and R magnitudes vs. longitudinal phase angle) for all data for each object separately. Once again, we use a human interface at this stage in order to further reject any possible spurious magnitude determinations. In Phase 1, there would typically be hundreds of spurious points in all the data for one object, but at the beginning of Phase 3, there are typically fewer than 10 and

---

<sup>2</sup> The software can be found at [www.astromatic.net/software](http://www.astromatic.net/software). It was written by E. Bertin (University of Paris).

<sup>3</sup> [www.stsci.edu/institute/software\\_hardware/pyraf](http://www.stsci.edu/institute/software_hardware/pyraf)

no spurious points are generally advanced past this stage. The user also can apply Expertise-based knowledge to assess whether or not to exclude whole regions within the signatures because of suspected sporadic clouds.

## 2.5 Photometric Error Estimation

In the current photometric catalog, we include uncertainty estimates for each new magnitude observation. We distinguish between two kinds of uncertainties.

For intra-day uncertainties, we use an estimate of the standard deviation of magnitude measurements that apply to observations taken for one sensor during a single night. Clearly, inter-comparisons of such magnitudes are not highly dependent on nightly calibration issues. For inter-day uncertainties, we use an estimate of the standard deviation of magnitude measurements that apply to observations taken by different sensors or by a single sensor but on different nights.

We find that the current photometric catalog has intra-day uncertainties of about  $\pm 0.10$  to  $\pm 0.15$  magnitudes, depending upon the sensor, the atmospheric conditions, and the quality of the calibration star observations. Similarly, the inter-day uncertainties are estimated to lie in the  $\pm 0.12$  to  $\pm 0.30$  range.

It is of interest to note that the uncertainties in the catalog grew when more automation was added to the processing. With the earlier and more manually intensive techniques, the errors were lower ( $\pm 0.05$  to  $\pm 0.08$  magnitudes for both intra-day and inter-day uncertainties) than the errors with the more recent semi-automated processing. The reasons for this are that we had much tighter control over the earlier collections than we now do. A somewhat higher uncertainty is one price that is paid for higher levels of automation and for use of multiple sensors in a wide network.

## 2.6 Examples of Satellite Photometry

In Fig. 4 and Fig. 5, there are examples of color photometry signatures for a 3-axis stabilized geostationary satellite. The data were taken with a small telescope on 01 March 2012. The concept of “signature” is applied to a plot of either magnitude (Fig. 4) or color index (Fig. 5) as a function of Longitudinal Phase Angle. Note the central brightening of the magnitude signatures in B and R (Fig. 4) near the time when the East-West component of the sun/satellite/sensor angle is zero – i.e.  $PA = 0^\circ$ . Also note the central obscuration seen as the Earth’s shadow crossed the satellite near  $PA = 0^\circ$ . In the color index signature (Fig. 5), the central brightening is seen to be significantly bluer (smaller value of B-R). This is characteristic of nearly specular reflections from most solar panels. Our primary purpose in presenting these two plots is to demonstrate the usefulness of photometric observations having accuracies of  $\pm 0.2$  magnitudes or less since some of the minor features in the brightness signatures would not be detectable with higher uncertainty. Such minor brightenings and dimmings can have important consequences in the analysis process.

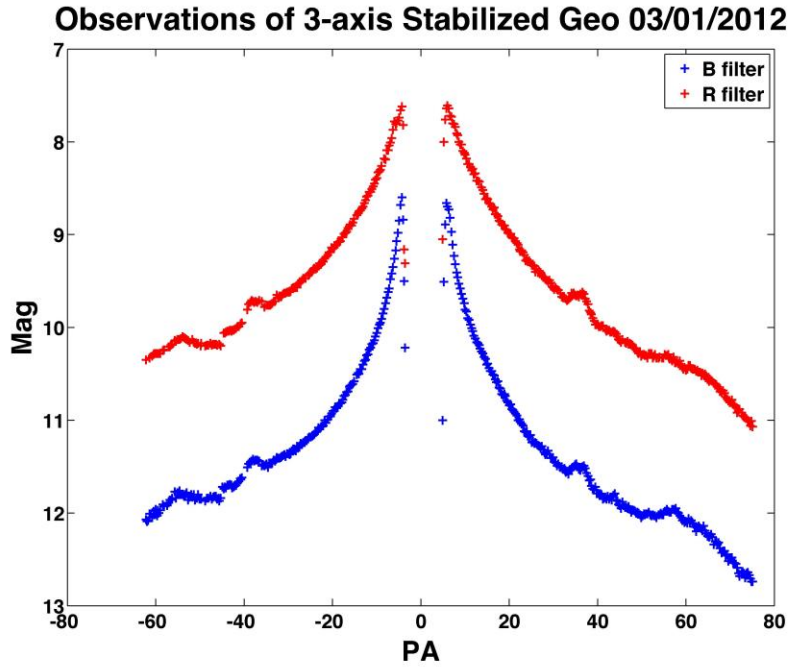


Fig. 4 Johnson B and R signatures (Magnitude vs. Longitudinal Phase Angle) for a 3-axis stabilized Geo satellite observed with a small telescope

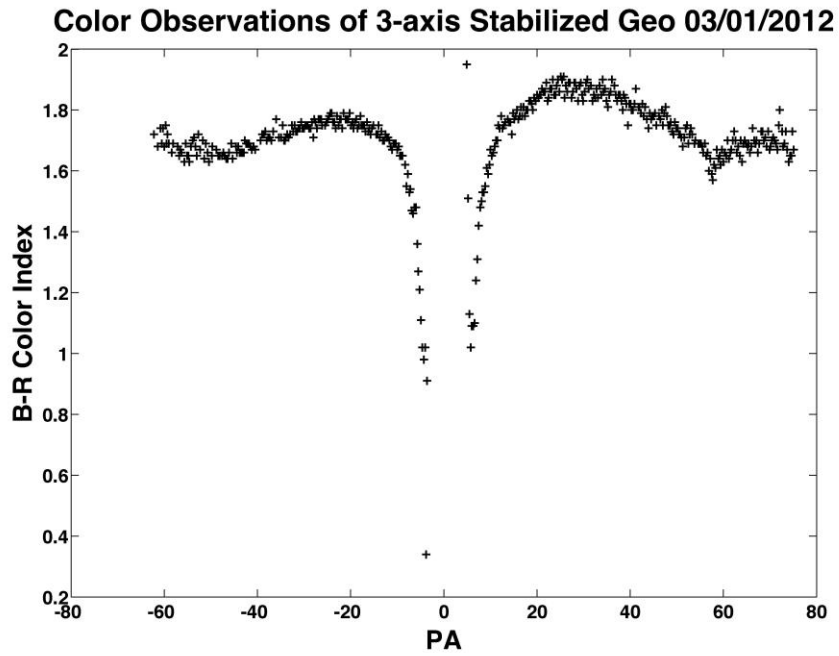


Fig. 5 B-R color index signature as a function of Longitudinal Phase Angle

### 3. FUTURE CONCEPT FOR THE STANDARDIZATION OF ACCURATE FILTER PHOTOMETRY

What lies ahead for the SSA community in the realm of improving photometric accuracies? There are two separate issues – in-frame calibrations and choice of filter systems. Clearly, in-frame calibrators would allow more accurate calibrations for atmospheric conditions that may change throughout the night and therefore are preferable when compared to all-sky calibrations.

The use of all-sky calibrations could, in fact, be accomplished with the commonly used Johnson filter system via use of the USNO B catalog, which is a very large collection of magnitudes in various optical band passes. This catalog is based on digitized scans of photographic plates that use emulsions whose band passes are close to some but not all of the Johnson photometric band passes (BVRI). However, the USNO B catalog is not the solution to the problem since it only has a photometric uncertainty of  $\pm 0.3$  magnitudes [24]. The sky coverage of the USNO B catalog is sufficient for in-frame calibrations, but the large uncertainty in photometry makes the catalog unsuitable to achieve calibrated photometry with low uncertainties.

The goal of achieving in-frame calibrations has become more nearly attainable by switching from the Johnson system. The astronomical community is tending to replace the Johnson filters with the Sloan filters [25] as the primary photometric system for optical observations. The most recent large astronomical surveys in the optical regime use the Sloan filters, beginning with the Sloan Digital Sky Survey (SDSS) [26] [27] that introduced the Sloan photometric system [25], and most recently with the Panoramic Survey Telescope and Rapid Response System (Pan-STARRS) [28] [29]. Both of these surveys use what is generally referred to as the Sloan photometric system, although individual differences exist between the filters used by SDSS and those used by Pan-STARRS [28].

Unfortunately, switching to the Sloan filters is not without problems in that it has not yet been demonstrated that the Sloan system provides satellite discrimination using color indices, as has been demonstrated with the Johnson system [12]. If the Sloan photometric system does provide discrimination of satellites akin to that of the Johnson photometric system then satellites observations in the Sloan photometric system becomes a viable option.

Let us examine the sky coverage of the Sloan observations. The SDSS does not have complete coverage of the celestial equator and the northern hemisphere [27], and therefore would not provide a complete solution for in-frame calibration stars. The Pan-STARRS 1 (PS1) project is surveying the  $3\pi$  steradians north of  $-30$  degrees declination. A major goal of the survey is to construct a precision photometry reference catalog covering the entire  $3\pi$  region [29]. The PS1 filters are  $g_{P1}$ ,  $r_{P1}$ ,  $i_{P1}$ ,  $z_{P1}$ ,  $y_{P1}$ , with the subscript to distinguish the PS1 photometric system from others. The PS1 photometry system is similar to the SDSS photometric system, but with a few differences. The  $g_{P1}$  filter extends 20 nm redward of the  $g_{SDSS}$  filter, the  $z_{P1}$  filter is cut off at 920 nm giving a different response from that for the  $z_{SDSS}$  filter, and SDSS has no corresponding  $y_{P1}$  filter [28]. The PS1 catalog covers the northern hemisphere and the southern hemisphere down to  $-30$  degrees declination. This coverage, in addition to the precision photometry, makes it well suited to serve as a catalog for in-frame calibrations for satellite observations.

A consequence of transitioning from the Johnson system to the Sloan system is that the catalogs of GEO satellite photometry using the Johnson photometric system discussed in Section 2 might become obsolete. In order for the historical data to not become obsolete, it would be important to transform the satellite photometry from the Johnson to the Sloan system. A number of such transformations exist [25] [30] [31] [32] [33] [34]. However, the transformations are based on stars not satellites, i.e. stellar spectral energy distributions and not satellite spectral energy distributions. It is not apparent that these transformations are valid for satellites. The validity would need to be investigated, and if not valid, then a transformation between Johnson and Sloan for satellites would need to be developed. A transformation for satellites would be more complicated than a transformation for stars because the spectral energy distribution of satellites can change with phase angle and is subject to specular features from solar panels, while the spectral energy distribution of calibration stars is stable.

A second option would be to continue using the Johnson photometric system for satellite observations, and transform stars from the PS1 catalog to the Johnson photometric system in order to perform in-frame calibrations.

This would enable continued use of the catalog of GEO satellite photometry. The second option still presents some issues. With the PS1 catalog used for in-frame calibrations after transforming from the PS1 photometric system to the Johnson photometry system, this transformation will introduce noise into the photometry of the in-frame calibration stars. The noise produced by the transformation is of significant importance if the goal is accurate photometry on a standard system. If the accuracy of the transformation is lower than the accuracy of the PS1 catalog, then the accuracy of the calibrations will be limited by the uncertainty of the transformation rather than that of the PS1 catalog. The noise introduced by the transformation needs to be characterized since this may place a limit on the accuracy of the calibrations. If the calibrations are of a lower accuracy than the instrumental photometry of the satellite, then the calibrations will place a limit on the photometric accuracy of satellite photometry in the Johnson system. The source of largest uncertainty determines the limit of accuracy of the satellite photometry. Tonry et al. provide transformations between the PS1 photometric system and the Johnson-Cousins photometric system [28]. Uncertainty values are provided for the color transformations from PS1 to the Johnson-Cousins photometric system. For the linear transformations these uncertainties are  $\pm 0.034$ ,  $\pm 0.012$ ,  $\pm 0.015$ , and  $\pm 0.016$ , for the  $B-g_{P1}$ ,  $V-r_{P1}$ ,  $R_c-r_{P1}$ , and  $I_c-i_{P1}$  transformation, respectively. Except for the transformation containing the B band, these are all at the 0.01 to 0.02 level. These transformations are derived from synthetic magnitudes from the spectral energy distributions of spectrophotometric standards from a variety of sources [28]. The uncertainty provided by the color transformations of Tonry et al. suggest that the uncertainty may be small enough to permit sufficiently high accuracy photometry of satellites on the Johnson photometric system using stars from the PS1 catalog and transforming them to the Johnson photometric system for in-frame calibrations [28]. In order to directly characterize the uncertainty in the transformed magnitudes from the PS1 photometric system to the Johnson photometric system for the purpose of in-frame calibrations of observations of satellites with Johnson filters, an empirical comparison of measured Johnson-Cousins photometry to the transformed Johnson-Cousins photometry for standard stars is performed.

#### 4. ANALYSIS

In this section, we will present work that shows how measurements using the Sloan filters might be used to continue SSA analyses in the Johnson system. We performed a search of the PS1 Photometric Reference Ladder, Release 12.01 for Landolt standard stars [29]. It is the first of a series of data releases of the PS1  $3\pi$  Survey to be generated as the survey coverage increases and the data analysis improves. The full PS1 catalog has not yet been released. The PS1 Photometric Reference Ladder has rungs every hour in right ascension and at four intervals in declination; it presents photometry of  $\sim 1000$  objects per square degree in the rungs of the ladder. Fig. 6 shows an illustration of the coverage of the Reference Ladder on the sky over a density plot of the PS1 catalog. The high density region is the galactic plane. There are two sets of photometry tables released, an Ubercal version and a relative photometry version (Relphot). The Ubercal version depends on the rigid Ubercal photometric calibration using only the photometric nights, with systematic uncertainties of  $g_{P1} = \pm 0.0080$ ,  $r_{P1} = \pm 0.0070$ ,  $i_{P1} = \pm 0.0090$ ,  $z_{P1} = \pm 0.0107$ ,  $y_{P1} = \pm 0.0124$  magnitudes. The relative photometry version consists of the Ubercal version plus relative photometry for areas covered only with lower quality nights, whose photometry is tied to the Ubercal solution via relative photometry. A compilation of Landolt stars from the celestial equator (2009) and the northern hemisphere (2013) were used as the Landolt standard stars for this analysis [10] [11]. The Landolt catalogs from 2009 and 2013 were trimmed as suggested by the author in order to ensure only standard stars were included. Landolt suggests using as standard stars those objects with the ‘number of observations’  $\geq 5$  and those with small errors. The ‘number of observations’ represents the number of times that a star was observed, while the error given in the catalog is the ‘mean error of the mean’. We trimmed each Landolt catalog to include only stars with ‘number of observations’  $\geq 5$  and those stars with errors  $< 0.02$  in the V magnitude and in the colors, B-V, V-R, R-I, and V-I. After one final step of removing stars from the Selected Area 95 (SA 95), this resulted in a size for the catalog of 590 stars.

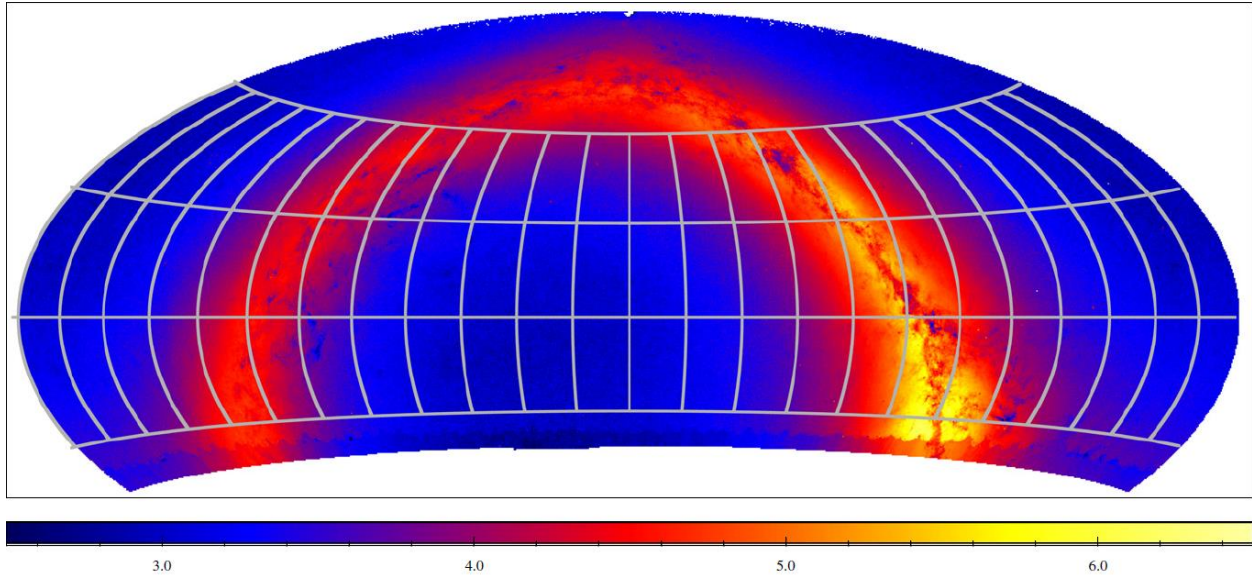


Fig. 6 Location of the PS1 Photometric Reference Ladder overlaid on a plot of the spatial density of objects from the PS1 catalog. The color scale gives the logarithm of the number of objects per square degree with at least three measurements and  $r_{p1} < 19.0$ . R. A. = 0.0 is at the center of the plot and increases to the left. From [29].

Using the Ubercal version of the PS1 Photometric Reference Ladder, Release 12.01, we searched for Landolt stars using a box of two arcseconds on a side centered on the Right Ascension and Declination of the Landolt stars. This search yielded only three matches, with this small number resulting from the fact that the PS1 Photometric Reference Ladder is an initial release. Using the linear transformations from the PS1 photometric system to the Johnson-Cousins photometric system [28], the PS1 photometry of the three Landolt stars was transformed to the Johnson-Cousins photometric system. We note that an additional search using the relative photometry version of the PS1 Photometric Reference Ladder did not yield any additional Landolt standard stars.

Fig. 7 shows the results. It is a plot of the measured Johnson-Cousins photometry versus the transformed Johnson-Cousins photometry for the B, V, R, and I bands. The colored circles represent the measured/transformed magnitudes, and the dashed line represents a slope of one through the origin, representing a perfect transformation. The root-mean-square (RMS) deviation [35] [36] of the transformed magnitude from the measured magnitude is shown for the B, V, R, and I bands. The deviation of the transformed magnitudes from the dashed line is small for all of the plots; except for one of the I band transformations, which is an outlier. The reason for the transformed I band data point being so large is unclear.

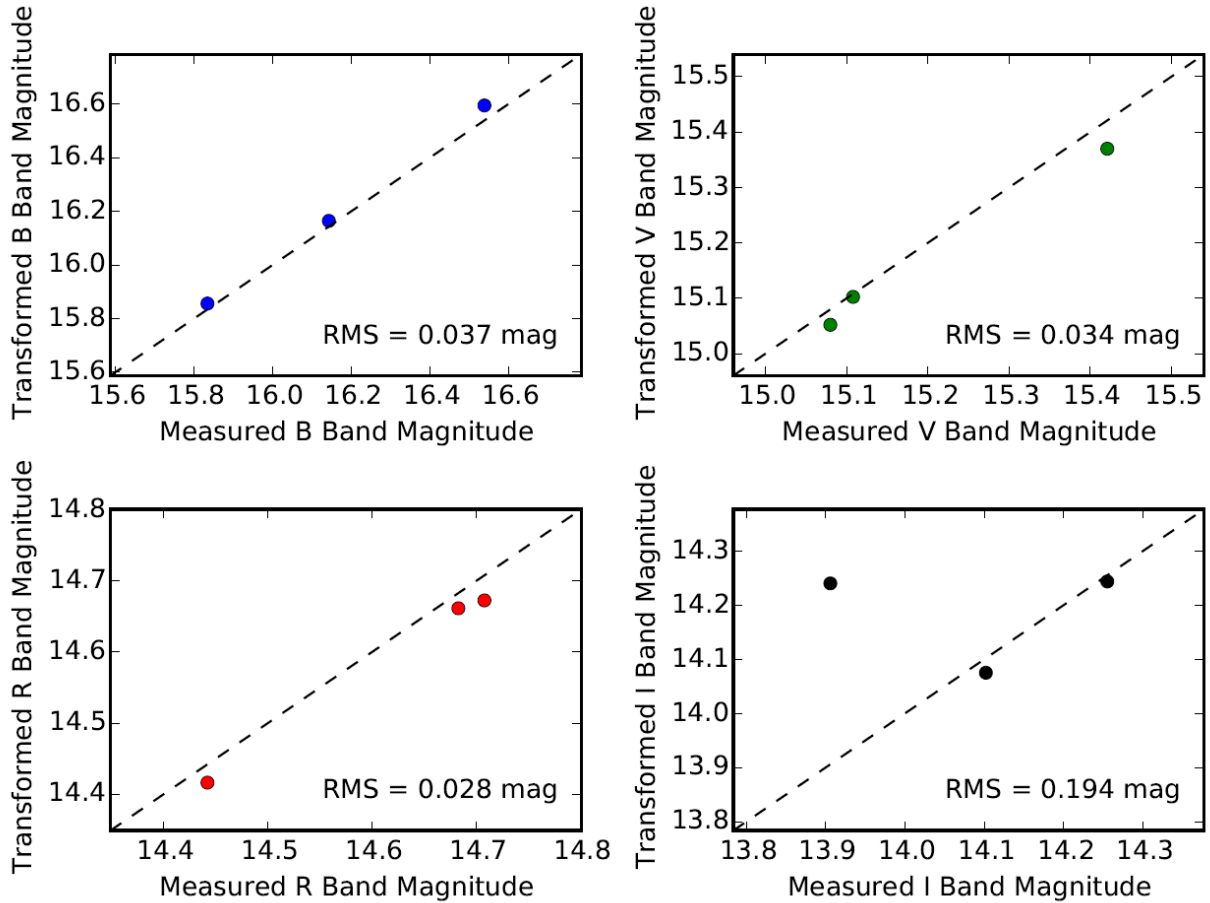


Fig. 7 Measured Johnson-Cousins photometry versus transformed Johnson-Cousins photometry for the B, V, R, and I bands

Tab. 1 below shows the properties of the stars used in the transformation analysis. It contains the star names from the 2009 and 2013 Landolt catalogs along with the right ascension and declination from these catalogs and the PS1 catalog, the total angular separation between the Landolt position and the PS1 position, and the measured, transformed, and absolute magnitude of their difference for the B, V, R, and I bands. The star names were modified to be consistent with SIMBAD<sup>4</sup> [37]. The total angular separation can provide a level of confidence in the matching between the Landolt star and the PS1 catalog. All of the total angular separations are below 1 arcsecond, with the largest about 0.5 arcseconds. The three stars were viewed in the Aladin Sky Atlas<sup>5</sup>; there was no other apparent source in the optical SDSS image within about five arcseconds of the Landolt positions. The close proximity of the Landolt position to the PS1 position and visual verification of there being no other star nearby provide additional confidence that the PS1 source matched to the Landolt position is indeed the Landolt standard star and not some other PS1 source near the Landolt star. Tab. 2 below shows the RMS deviation of the transformed magnitude from the measured magnitude for the B, V, R, and I bands. All of the uncertainties are less than  $\pm 0.04$  magnitudes except for the I band due to the outlier.

<sup>4</sup> <http://simbad.u-strasbg.fr/simbad/>

<sup>5</sup> <http://aladin.u-strasbg.fr/aladin.gml>

Tab. 1. Properties of Stars used in Transformation Analysis

|                          |               |            |            |
|--------------------------|---------------|------------|------------|
| Star Name                | PG 2213-006 C | SA 113-187 | SA 113-189 |
| R.A. Landolt (deg)       | 334.073642    | 325.835954 | 325.864504 |
| Dec. Landolt (deg)       | -0.370639     | 0.281728   | 0.289142   |
| R.A. PS1 (deg)           | 334.073631    | 325.835992 | 325.864409 |
| Dec. PS1 (deg)           | -0.370656     | 0.281744   | 0.289034   |
| Total Ang. Sep. (arcsec) | 0.073         | 0.146      | 0.520      |
| B Measured (mag)         | 15.834        | 16.143     | 16.539     |
| B Transformed (mag)      | 15.856        | 16.164     | 16.595     |
| $ \Delta B $ (mag)       | 0.022         | 0.021      | 0.056      |
| V Measured (mag)         | 15.108        | 15.08      | 15.421     |
| V Transformed (mag)      | 15.103        | 15.052     | 15.370     |
| $ \Delta V $ (mag)       | 0.005         | 0.028      | 0.051      |
| R Measured (mag)         | 14.683        | 14.442     | 14.708     |
| R Transformed (mag)      | 14.662        | 14.416     | 14.673     |
| $ \Delta R $ (mag)       | 0.021         | 0.026      | 0.035      |
| I Measured (mag)         | 14.255        | 13.906     | 14.102     |
| I Transformed (mag)      | 14.244        | 14.240     | 14.075     |
| $ \Delta I $ (mag)       | 0.011         | 0.334      | 0.027      |

Tab. 2. RMS from Transformation

|           |       |       |       |       |
|-----------|-------|-------|-------|-------|
|           | B     | V     | R     | I     |
| RMS (mag) | 0.037 | 0.034 | 0.028 | 0.194 |

This analysis shows that the uncertainty introduced by the transformation from the PS1 photometric system to the Johnson-Cousins photometric system is small,  $RMS < 0.04$  magnitudes; except for the I band due to an outlier. Excluding the “bad” I band data point, the deviation of the transformed I band magnitudes from the measured I band magnitudes is similar to the other bands. The RMS of the transformed Landolt star magnitudes from the measured Landolt star magnitudes provides an empirical determination of the uncertainty introduced using traditional Johnson-Cousins calibration stars and characterizes the validity of using the PS1 catalog for in-frame calibrations in the Johnson-Cousins photometric system via a transformation from PS1 to Johnson-Cousins. The results suggest that the proposed technique will be capable of providing accurate photometry of satellites observed in the Johnson-Cousins photometric system. With only three stars for analysis, the results are suggestive but far from conclusive. Upon the full release of the PS1 catalog, this analysis should be repeated, with the expectation that virtually all of the Landolt standard stars will be found in the PS1 catalog. With hundreds of Landolt stars to compare the measured Johnson-Cousins photometry to the transformed Johnson-Cousins photometry, a complete analysis will provide conclusive and robust statistical results.

## 5. CONCLUSIONS

We have presented discussions of calibrations and uncertainties for photometric observations in the visible wavelength regions and have shown how current SSA observations differ from standard astronomy community practices. An important concept in the near future is how to improve techniques while maintaining or improving accuracies. Higher accuracy photometry can be achieved through a standardization of calibrations, especially the choice of standard star catalog. In-frame photometric calibration can be achieved through the use of PS1. Preliminary results show that the uncertainties introduced by transforming from Sloan to Johnson appear to be small enough, i.e.  $\pm 0.05$  to  $\pm 0.10$  magnitudes, to achieve calibrated photometry on a standard scale (Johnson) of the order  $\pm 0.10$  magnitudes. Therefore, it appears that this will not be the dominant source of error. Additional work should be done after the full release of PS1. The most crucial question to answer is if the Sloan band passes will afford adequate discrimination among satellites based on color indices. Moving forward, the discrimination by Sloan needs to be determined in order to make a final determination on a standardized filter set for SSA.

## 6. ACKNOWLEDGEMENTS

The Pan-STARRS1 Surveys (PS1) have been made possible through contributions of the Institute for Astronomy, the University of Hawaii, the Pan-STARRS Project Office, the Max-Planck Society and its participating institutes, the Max Planck Institute for Astronomy, Heidelberg and the Max Planck Institute for Extraterrestrial Physics, Garching, The Johns Hopkins University, Durham University, the University of Edinburgh, Queen's University Belfast, the Harvard-Smithsonian Center for Astrophysics, the Las Cumbres Observatory Global Telescope Network Incorporated, the National Central University of Taiwan, the Space Telescope Science Institute, the National Aeronautics and Space Administration under Grant No. NNX08AR22G issued through the Planetary Science Division of the NASA Science Mission Directorate, the National Science Foundation under Grant No. AST-1238877, the University of Maryland, and Eotvos Lorand University (ELTE). This research has made use of the SIMBAD database, operated at CDS, Strasbourg, France. This research has made use of "Aladin sky atlas" developed at CDS, Strasbourg Observatory, France.

## REFERENCES

- [1] H. L. Johnson and W. W. Morgan, "Fundamental Stellar Photometry for Standards of Spectral Type on the Revised System of the Yerkes Spectral Atlas," *The Astrophysical Journal*, vol. 117, pp. 313-352, 1953.
- [2] H. L. Johnson, R. I. Mitchell, B. Iriarte and W. Z. Wisniewski, "UBVRIJKL Photometry of the Bright Stars," *Communications of the Lunar and Planetary Laboratory*, vol. 4, p. 99, 1966.
- [3] M. S. Bessell, "Standard Photometric Systems," *Annual Review of Astronomy & Astrophysics*, vol. 43, pp. 293-336, 2005.
- [4] G. E. Kron, H. S. White and S. C. B. Gascoigne, "Red and Infrared Magnitudes for 138 Stars Observed as Photometric Standards," *The Astrophysical Journal*, vol. 118, pp. 502-510, 1953.
- [5] A. W. J. Cousins, "VRI Standards in the E Regions," *Memoirs of the Royal Astronomical Society*, vol. 81, pp. 25-36, 1976.
- [6] A. U. Landolt, "UBVRI Photometric Standard Stars Around the Celestial Equator," *The Astronomical Journal*, vol. 88, pp. 439-460, 1983.
- [7] A. U. Landolt, "UBV Photoelectric Sequences in the Celestial Equatorial Selected Areas," *The Astronomical Journal*, vol. 78, pp. 959-1021, 1973.

- [8] B. D. Warner, *A Practical Guide to Lightcurve Photometry and Analysis*, New York: Springer, 2006.
- [9] A. U. Landolt, "UBVRI Photometric Standard Stars in the Magnitude Range  $11.5 < V < 16.0$  Around the Celestial Equator," *The Astronomical Journal*, vol. 104, pp. 340-491, 1992.
- [10] A. U. Landolt, "UBVRI Photometric Standard Stars Around the Celestial Equator: Updates and Additions," *The Astronomical Journal*, vol. 137, pp. 4186-4269, 2009.
- [11] A. U. Landolt, "UBVRI Photometric Standard Stars Around the Sky at +50 deg Declination," *The Astronomical Journal*, vol. 146, p. 131, 2013.
- [12] T. E. Payne, S. A. Gregory, D. J. Sanchez, L. G. Finkner, D. M. Payne, L. Kann, C. K. Davis and D. Werling, "Space Object Identification of Geosynchronous Satellites," in *AMOS Technical Conference*, 1999.
- [13] T. E. Payne, S. A. Gregory, J. Tombasco, K. Luu and L. Durr, "Satellite Monitoring, Change Detection, and Characterization Using Non-Resolved Electro-Optical Data from a Small Aperture Telescope," in *AMOS*, 2007.
- [14] P. B. Stetson, "Homogeneous Photometry for Star Clusters and Resolved Galaxies. II. Photometric Standard Stars," *Publications of the Astronomical Society of the Pacific*, vol. 112, pp. 925-931, 2000.
- [15] D. A. Simons and A. Tokunaga, "The Mauna Kea Observatories Near-Infrared Filter Set. I. Defining Optimal 1-5 Micron Bandpasses," *Publications of the Astronomical Society of the Pacific*, vol. 114, pp. 169-179, 2002.
- [16] A. T. Tokunaga, D. A. Simons and W. D. Vacca, "The Mauna Kea Observatories Near-Infrared Filter Set. II. Specifications for a New JHKLM' Filter Set for Infrared Astronomy," *Publications of the Astronomical Society of the Pacific*, vol. 114, pp. 180-186, 2002.
- [17] A. T. Tokunaga and W. D. Vacca, "The Mauna Kea Observatories Near-Infrared Filter Set. III. Isophotal Wavelengths and Absolute Calibration," *Publications of the Astronomical Society of the Pacific*, vol. 117, pp. 421-426, 2005.
- [18] T. Payne, S. Gregory, D. Sanchez, L. Finkner, D. Payne, L. Kann and C. Davis, "Space Object Identification of Geosynchronous Satellites," in *AMOS Technical Conference*, Wailea, 1999.
- [19] T. Payne, S. Gregory, D. Sanchez, T. Burdullis and S. Storm, "Color Photometry of Geosynchronous Satellites Using the SILC Filters," *SPIE Multifrequency Electronic/Photonic Devices and Systems for Dual-Use Applications*, vol. 4490, 2001.
- [20] T. E. Payne, S. A. Gregory, N. M. Houtkooper and T. W. Burdullis, "Analysis of Multispectral Radiometric Signatures from Geosynchronous Satellites," *SPIE Astronomical Data Analysis II*, vol. 4847, 2002.
- [21] T. Payne, S. Gregory and N. Houtkooper, "Long-Term Analysis of GEO Photometric Signatures," in *AMOS Technical Conference*, Wailea, 2003.
- [22] T. Payne, S. Gregory, F. Vrba and K. Luu, "Utility of a Multi-Color Photometric Database," in *AMOS Technical Conference*, Wailea, 2005.
- [23] T. Payne, S. Gregory and K. Luu, "Electro-optical signatures comparisons of geosynchronous satellites," in *IEEE Aerospace Conference*, Big Sky, 2006.
- [24] D. G. Monet, S. E. Levine, B. Canzian, H. D. Ables, A. R. Bird, C. C. Dahn, H. H. Guetter, H. C. Harris, A. A. Henden, S. K. Leggett, H. F. Levison, C. B. Luginbuhl, J. Martini and A. K. B. Monet, "The USNO-B Catalog," *The Astronomical Journal*, vol. 125, pp. 984-993, 2003.

- [25] M. Fukugita, T. Ichikawa, J. E. Gunn, M. Doi, K. Shimasaku and D. P. Schneider, "The Sloan Digital Sky Survey Photometric System," *The Astronomical Journal*, vol. 111, pp. 1748-1756, 1996.
- [26] D. G. York, J. Adelman, J. E. Anderson Jr., S. F. Anderson, J. Annis, N. A. Bahcall, J. A. Bakken, R. Barkhouser, S. Bastian, E. Berman, W. N. Boroski, S. Bracker, C. Briegel and J. W. Briggs, "The Sloan Digital Sky Survey: Technical Summary," *The Astronomical Journal*, vol. 120, pp. 1579-1587, 2000.
- [27] K. N. Abazajian, J. K. Adelman-McCarthy, M. A. Agüeros, S. S. Allam, C. A. Prieto, D. An, K. S. J. Anderson, S. F. Anderson, J. Annis, N. A. Bahcall, C. A. L. Bailer-Jones and J. C. Barentine, "The Seventh Data Release of the Sloan Digital Sky Survey," *The Astrophysical Journal Supplement Series*, vol. 182, pp. 543-558, 2009.
- [28] J. L. Tonry, C. W. Stubbs, K. R. Lykke, P. Doherty, I. S. Shivvers, W. S. Burgett, K. C. Chambers, K. W. Hodapp, N. Kaiser, R. P. Kudritzki, E. A. Magnier, J. S. Morgan, P. A. Price and R. J. Wainscoat, "The Pan-STARRS1 Photometric System," *The Astrophysical Journal*, vol. 750, p. 99, 2012.
- [29] E. A. Magnier, E. Schlafly, D. Finkbeiner, M. Juric, J. L. Tonry, W. S. Burgett, K. C. Chambers, H. A. Flewelling, N. Kaiser, R. P. Kudritzki, J. S. Morgan, P. A. Price, W. E. Sweeney and C. W. Stubbs, "The Pan-STARRS 1 Photometric Reference Ladder, Release 12.01," *The Astrophysical Journal Supplement Series*, vol. 205, p. 20, 2013.
- [30] J. A. Smith, D. L. Tucker, S. Kent, M. W. Richmond, M. Fukugita, T. Ichikawa, S.-I. Ichikawa, A. M. Jorgensen, A. Uomoto, J. E. Gunn, M. Hamabe, M. Watanabe, A. Tolea and A. Henden, "The u'g'r'i'z' Standard-Star System," *The Astronomical Journal*, vol. 123, pp. 2121-2144, 2002.
- [31] S. Jester, D. P. Schneider, G. T. Richards, R. F. Green, M. Schmidt, P. B. Hall, M. A. Strauss, D. E. Vanden Berk, C. Stoughton, J. E. Gunn, J. Brinkmann, S. M. Kent and J. A. Smith, "The Sloan Digital Sky Survey View of the Palomar-Green Bright Quasar Survey," *The Astronomical Journal*, vol. 130, pp. 873-895, 2005.
- [32] J. R. A. Davenport, A. A. West, C. K. Matthiesen, M. Schmieding and A. Kobelski, "Sloan/Johnson-Cousins/2MASS Color Transformations for Cool Stars," *Publications of the Astronomical Society of the Pacific*, vol. 118, pp. 1679-1684, 2006.
- [33] C. T. Rodgers, R. Canerna, J. A. Smith, M. J. Pierce and D. L. Tucker, "Improved u'g'r'i'z' to UBVRcIc Transformation Equations for Main-Sequence Stars," *The Astronomical Journal*, vol. 132, pp. 989-993, 2006.
- [34] K. Jordi, E. K. Grebel and K. Ammon, "Empirical Color Transformations between SDSS Photometry and other Photometric Systems," *Astronomy & Astrophysics*, vol. 460, pp. 339-347, 2006.
- [35] J. V. Wall and C. R. Jenkins, *Practical Statistics for Astronomers*, Second ed., Cambridge: Cambridge University Press, 2012.
- [36] W. Lichten, *Data and Error Analysis*, Second ed., Upper Saddle River: Prentice Hall, 1999.
- [37] M. Wenger, F. Ochsenbein, D. Egret, P. Dubois, F. Bonnarel, S. Borde, F. Genova, G. Jasniewicz, S. Laloe, S. Lesteven and R. Monier, "The SIMBAD Astronomical Database," *Astronomy & Astrophysics Supplement Series*, vol. 143, pp. 9-22, 2000.